CELL CYCLE
2020, VOL. 19, NO. 2, 179–192
https://doi.org/10.1080/15384101.2019.1704512

Taylor & Francis
Taylor & Francis Group

RESEARCH PAPER



# Downregulation of miR-155-5p facilitates enterovirus 71 replication through suppression of type I IFN response by targeting FOXO3/IRF7 pathway

Daokun Yang, Xinwei Wang, Haili Gao, Baoxin Chen, Changyun Si, and Shasha Wang

Department of Infectious Disease III, The First Affiliated Hospital of Xinxiang Medical University, Weihui, China

**ABSTRACT**

Enterovirus 71 (EV71), the major cause of hand-foot-and-mouth disease (HFMD), has evolved diverse strategies to counter the type I interferon (IFN-I) response during infection. Recently, microRNAs have regulatory roles in host innate immune responses to viral infections; however, whether EV71 escapes the IFN-I antiviral response through regulation of miRNAs remains unclear. Using a microarray assay, microRNA-155-5p (miR-155-5p) was found to be significantly up-regulated in serum from patients with EV71 infection and the increased expression of miR-155-5p was further confirmed *in vivo* and *in vitro* in response to EV71 infection. miR-155-5p overexpression suppressed EV71 titers and VP1 protein level, while miR-155-5p inhibition had an opposite result. Moreover, we found that miR-155-5p overexpression enhanced EV71 triggered IFN I production and the expressions of IFN-stimulated genes (ISGs), while inhibition of miR-155-5p suppressed these processes. Furthermore, bioinformatics analysis and luciferase reporter assay demonstrated that miR-155-5p directly targeted forkhead box protein O3 (FOXO3) and negatively regulated FOXO3/IRF7 axis, an important regulatory pathway for type I IFN production during EV71 infection. Inhibition of FOXO3 reversed the effects of miR-155-5p inhibitor on EV71 replication and the type I IFN production. Importantly, in EV71 infection mice, agomir-155-5p injection resulted in a significant reduction of viral VP1 protein expressions in brain and lung tissues, increased IFN-α/β production and increased mice survival rate. In contrast, antagomir-155-5p enhanced EV71 induced these effects. Collectively, our study indicates that weaken miR-155-5p facilitates EV71 replication through suppression of type I IFN response by FOXO3/IRF7 pathway, thereby suggesting a novel strategy for developing effective antiviral therapy.

**ARTICLE HISTORY**
Received 30 August 2019
Revised 29 October 2019
Accepted 13 November 2019

**KEYWORDS**
Enterovirus 71; miR-155-5p; FOXO3/IRF7 pathway

## Introduction

Enterovirus 71 (EV71) is one major causative pathogen of infant hand-foot-and-mouth disease (HFMD) and its infection can result in severe cerebral and pulmonary complications [1]. More than 7 million children suffered from HFMD from 2008 to 2012 and about 90% of the reported cases below 10 years old in China [2,3]. Despite some advances that have been made to improve the diagnosis and therapy of HFMD patients, all demonstrated limited efficacy thus far. Therefore, it has become extremely important to find novel means to completely suppress viral replication.

During viral infection, the innate immune response recognizes viral components and triggers downstream signal transduction, leading to the expression of type I interferons (IFNs) [4–6]. Binding of IFN-I to its receptor results in activation of JAK-STAT signaling cascades, consequently inducing more than 300 IFN-stimulated genes (ISGs) expressions, which directly inhibits viral replication and mediates protection against viral infection [7]. Several studies have demonstrated that Type I IFN could effectively prevent the host from EV71 infection [2,8,9]. Among the interferon regulatory factors (IRFs), IRF3 and IRF7, are key regulators in the host response against EV71 infection due to the induction of the IFN-α/β genes transcription [10,11]. Despite considerable understanding how EV71 triggers IFN-I production, how EV71 fights the antiviral activity of IFN-I remains to be fully elucidated.

MicroRNAs (miRNAs) are a family of short, small, noncoding RNAs (an average size of 22 nucleotides) that negatively regulate target gene expression through either translation repression or RNA degradation [12]. Increasing evidence has indicated host miRNAs participate in various types of virus infection through modulating type I IFNs [13,14]. For example, Ma et al. showed that suppression of miR-30a-5p facilitated TGEV

**CONTACT** Daokun Yang daokunyangdk@163.com

infection via modulation of IFN-I signaling by directly targeting the suppressor of cytokine signaling protein 1 (SOCS1), and SOCS3 [15]. Xie et al. demonstrated that miR-373 was a negative regulator of IFN-I response by directly targeting IRF1, resulting in the suppression of ISG expressions and enhancement of herpes simplex virus type 1 (HSV-1) infection [16]. For EV71, Feng et al. showed that miR-21 was upregulated in response to EV71 infection, and EV71 replication was enhanced by miR-21 through suppressing type I IFN production [17]. However, the underlying mechanism employed by EV71 to escape the IFN-I antiviral response via modulation of miRNAs remains largely unknown.

In the present study, we analyzed the expression profiles of miRNAs in serum samples from patients infected with EV71 using miRNA microarray, and found that miR-155-5p was significantly upregulated in the process. Furthermore, the influences of miR-155-5p on EV71 replication were examined, and the role of FOXO3/IRF7 pathway in miR-155-5p mediated type I IFN response and viral replication was confirmed *in vitro* and *in vivo*. Our data highlight the potential functions of miR-155-5p in the antiviral therapy for EV71 infection.

## Materials and methods

### Clinical samples

Twenty serum samples were obtained from patients with EV71 infection at the First Affiliated Hospital of Xinxiang Medical University from January 2017 to January 2018. Ten serum samples from healthy controls were used as negative controls. Serum samples were stored frozen at −20°C until analyzed. All experiments were approved by Research Ethics Committee of Xinxiang Medical University. Written informed consent was obtained from each patient or the parents of pediatric participants.

### Cell culture and transfection

Vero, RD, HT-29, HeLa, and THP-1 cells were maintained in Minimum essential medium (MEM; Gibco, Shanghai, China) supplemented with 10% (v/v) FBS (Gibco) plus 100 U/ml penicillin/streptomycin at 37°C and 5% $CO_2$ incubator.

When RD cells in six-well plate grown to about 80% confluence, miR-155-5p mimics, miR-155-5p inhibitor (20 nmol/L) or si-FOXO3 (30 nM) were transfected into RD cells at 37°C for 24 h, using Lipofectamine® 2000 (Invitrogen). miR-155-5p mimics, miR-155-5p inhibitor, the corresponding control vectors, FOXO3 small interfering (si)-RNA -1, −2, −3 and scramble siRNA were purchased from RiboBio Co., Ltd. (Guangzhou, China).

### Virus infection

A monolayer of RD cells in six-well plate were infected with EV71 strain (BrCr) (CCTC, Wuhan, China) at a multiplicity of infection (MOI) = 1 and incubated for 2 days. Virus stocks were assessed by $TCID_{50}$ assay and calculated according to Reed and Muench [18].

### Microarray assay

Total RNA from serum samples of EV71 infected patients and healthy controls were extracted using miRNeasy mini kit (Qiagen, West Sussex, UK). After quantitation by NanoDrop ND-1000 spectrophotometry (Thermo Fisher Scientific, Inc., Waltham, MA, USA), total RNA (200 ng) was labeled with fluorescence dye hy3 or hy5 using the miRCURY Hy3/Hy5 Power Labeling kit and hybridized on the miRCURY™ LNA array (v.16.0; Exiqon A/S, Copenhagen, Denmark), which were designed based on miRBaserelease 10.0 and contained 546 probes from humans, mice and rats. The procedure and imaging processes were as described previously [19].

### qRT-PCR

Total RNA from RD cells and serum samples were isolated by using TRIzol reagent (TaKaRa, Dalian, China). Reverse transcription of miR-155-5p and FOXO3 was synthesized using the miScript II RT kit and the reverse transcription kit (Invitrogen, Carlsbad, CA), respectively. miR-155-5p expression was detected by using the TaqMan miRNAs Quantitation kit (Applied Biosystems, Foster City, CA, USA) and FOXO3 expression was measured using the Exiqon SYBR Green Master Mix (Exiqon, Vedbaek, Denmark) on a Light Cycler instrument

(Bio-Rad). The primers for qRT-PCR analysis were as follows: miR-155-5p F: 5'-TTAATGCTA ATCGTGATAGGGGT-3'; miR-155-5p R: 5'-GCTGTCAACGATACGCTACGTAACG-3' U6 F: 5'-TGCGGGTGCTCGCTTCGCAGC-3'; U6 R: 5'-CCAGTGCAGGGTCCGAGGT-3'; ISG15 F: 5'-GGCTGGGAGCTGACGGTGAAG-3', ISG15 R: 5'-GCTCCGCCCGCCAGGCTCTGT-3'; OAS F: 5'-AGGTGGTAAAGGGTGGCT-3', OAS R: 5'-TG CTTGACTAGGCGGATG-3'; MxA F: 5'-GG GAAGGTGAAGGTCGGAGT-3', MxA R: 5'-TTGAGGTCAATGAAGGGGTCA-3'; PKR F: 5'-AGAGTAACCGTTGGTGACATAACCT-3', PKR R: 5'-GCAGCCTCTGCAGCTCTATGTT-3'; FO XO3 F: 5'-CTGGGGGAACCTGTCCTATG-3' FO XO3 R: 5'-TCATTCTGAACGCGCATGAAG-3'; GAPDH F: 5'-AGGTCGGTGTGAACGGATTTG-3', GAPDH R: 5'-TGTAGACCATGTAGTTG AGGTCA-3'. The relative expression of miRNA and mRNA was calculated using the $2^{-\Delta\Delta CT}$ method [20] and determined by normalization to U6 or GAPDH, respectively.

### ELISA

The concentrations of IFN-α (Catalog Number: CSB-E08636h; Cusabio, China) and IFN-β (Catalog Number: CSB-E09889h; Cusabio, China) levels in cell supernatants were determined by human ELISA kit according to the kit instructions. The concentrations of IFN-α (Catalog Number: 42120–1; PBL Interferon source, Piscataway, NJ, USA) and IFN-β (Catalog Number: 42400–1; PBL Interferon source, Piscataway, NJ, USA) levels in serum from mice were measured by mouse ELISA kits according to the kit instructions.

### Immunofluorescence (IFA)

After 24 h the EV71 infection, the cells fixed in absolute ethyl alcohol for 30 minutes at room temperature (RT). After washing twice with PBS, the fixed cells were stained with primary antibody EV71 VP1 prepared by our laboratory for 1 hour at RT. Then, the secondary antibody conjugated with FITC (1:100, Sigma-Aldrich, St Louis, MO) was added for 2 h in the dark, fluorescence images were collected and analyzed using an inverted fluorescence microscope.

### Dual-luciferase reporter assay

The dual-luciferase reporter assay was performed as described previously [21,22]. RD cells were co-transfected with miR-155-5p mimics, miR-155-5p inhibitor and the luciferase reporter plasmids using Lipofectamine 2000 (Invitrogen). At 24 h post-transfection, the double luciferase activities were analyzed using the Dual-Luciferase Reporter Assay system (Promega Corporation).

### Western blot

Western blot was performed as previously described [23]. Briefly, the extracted protein concentration was determined using a BCA kit (Beyotime Institute of Biotechnology, Haimen, China). 40 μg protein samples were resolved on 10% SDS-PAGE gels, transferred onto a polyvinylidene difluoride (PVDF, Millipore) membrane and then this membrane was blocked with 5% skim milk for 2 h at 4°C overnight, and probed with FOXO3 antibody (1:1,000; cat. no. 12162, Abcam), IRF7 antibody (1:1,000; cat. no. 115352, Abcam) and β-actin (1:2,000; cat. no. 179467; Abcam) overnight at 4°C, followed by HRP-conjugated goat anti-rabbit IgG (1:10,000; cat. no. 205718; Abcam). The protein bands were developed using ECL kit (GE Healthcare) and blot bands were quantified with ImageJ (version 1.46; Rawak Software, Inc. Munich, Germany).

### EV71 infection in mice and ethics statement

C57BL/6 mice (two-week-old female mice) were provided by Shanghai SLAC Laboratory Animal Co.,Ltd (Shanghai, China), housed under standard conditions (12h light-dark cycle, 25-27°C, ~40% humidity) with free access to food and water throughout the duration of the experiments. All animal procedures were approved by the Animal Ethics Committee of Xinxiang Medical University. A mouse-adapted EV71 strain (mEV71) was established as previously described [24]. All mice were randomly divided into four groups (n = 10/group): (1) Control group (2) EV71 group (3) EV71 + agomir-155-5p group, (4) EV71 + antagomir-155-5p group. In EV71 group, mice were injected with indicated PFUs of mEV71 through the oral route; and the control group was fed with culture medium. In agomir-155-5p or

antagomir-155-5p groups, mice were intraperitoneally injected with agomir-155-5p (1.2 mg/kg) or antagomir-155-5p (1.2 mg/kg) 24 h prior to EV71 injection. Mice were anesthetized with an intraperitoneal (i.p) injection of 3% chloral hydrate at 1, 3, 5 and 7d after EV71 infection except survival experiment, then the mice were sacrificed and the blood, brain, liver, spleen, lung, kidney, and muscle tissue of mice were collected for RNA extraction, in which brain and lung tissue of mice were harvested for immunohistochemistry. The survival rate was observed from 0 h to 96 h using the Kaplan Meier methods.

### Immunohistochemistry (IHC) staining

IHC staining was performed as previously described [25]. Briefly, brain and lung sections were deparaffinized and rehydrated, and antigen retrieval was conducted with Target Retrieval Solution (Dako, CA, USA). Endogenous peroxidase activity was blocked with 0.3% hydrogen peroxide for 15 min, followed incubation with rabbit anti-human polyclonal antibodies against VP1 (1:200 dilution) at 4 °C overnight and then probed with biotinylated goat anti-rabbit secondary antibody (Vector Laboratories, CA, USA) and high-sensitivity streptavidin–HRP conjugate. Images of IHC were photographed using an Olympus BX51 light microscope (Olympus Inc., Tokyo, Japan) at 200× magnification. ImageJ version 1.46 (Rawak Software, Inc. Munich, Germany) was used to quantify IHC staining.

### Statistical analysis

The difference between means was analyzed using Student´s t-test and analysis of variance (ANOVA) using SPSS 13.0 software package (SPSS Inc., Chicago, IL). All data are showed as the mean ± standard deviation (SD). P value less than 0.05 was considered statistically significant.

## Results

### miR-155-5p was up-regulated in response to EV71 infection

To evaluate miRNA expression profiles between serum samples from patients with EV71 infection and serum samples from healthy controls, a miRNA microarray assay was performed. Of 60 differently expressed miRNAs 26 miRNAs were downregulated and 34 miRNAs were upregulated in the EV71 infection group, compared with those in the healthy control group (Figure 1(a)). Among them, miR-155-5p displayed greatest fold-change in response to EV71 infection. In addition, miR-155-5p has also been found to be upregulated in myocardial tissues of patients with acute coxackievirus B3 (CVB3) virus infection [26]. Interestingly, several studies have shown that miR-155-5p acts as a suppressive regulator of virus replication in some viral diseases [27–30]. However, little attention has been paid on its function in EV71 infection. Therefore, miR-155-5p was selected for further investigation.

To validate the expression of miR-155-5p obtained from the miRNA microarray assay, the levels of miR-155-5p was detected by qRT-PCR in 20 serum samples from patients with EV71 and 10 serum samples from healthy controls. As shown in Figure 1(b), the expression of miR-155-5p was significantly increased in EV71 group, compared with control group. We also examined the miR-155-5p levels in several cell lines infected with EV71 by qRT-PCR. Consistent with the expression levels of miR-155-5p in the clinical samples, miR-155-5p was obviously increased in EV71 infected Vero, RD, HT-29, HeLa, and THP-1 cells, compared with that in control cells (uninfected cells), especially in RD cells (Figure 1(c)). Next, we measured the expression of miR-155-5p in RD cells infected with EV71 (MOI = 1) by qRT-PCR at different times. The level of miR-155-5p was increased at 4 h post-infection and the highest miR-155-5p levels was found at 24 h post-infection (Figure 1(d)). Furthermore, we found that the level of miR-155-5p was MOI-dependently increased in EV71-infected RD cells (Figure 1(e)).

### miR-155-5p regulated EV71 replication

To further examine the effect of miR-155-5p on EV71 replication, RD cells were transfected with miR-155-5p mimics and its inhibitor, and infected with EV71. As shown in Figure 2(a), miR-155-5p was significantly increased after miR-155-5p mimics transfection, but decreased after miR-155-5p inhibitor transfection in RD cells. Then, the EV71 virus titers in RD cells were analyzed at 4, 6, 12, and 24 h post

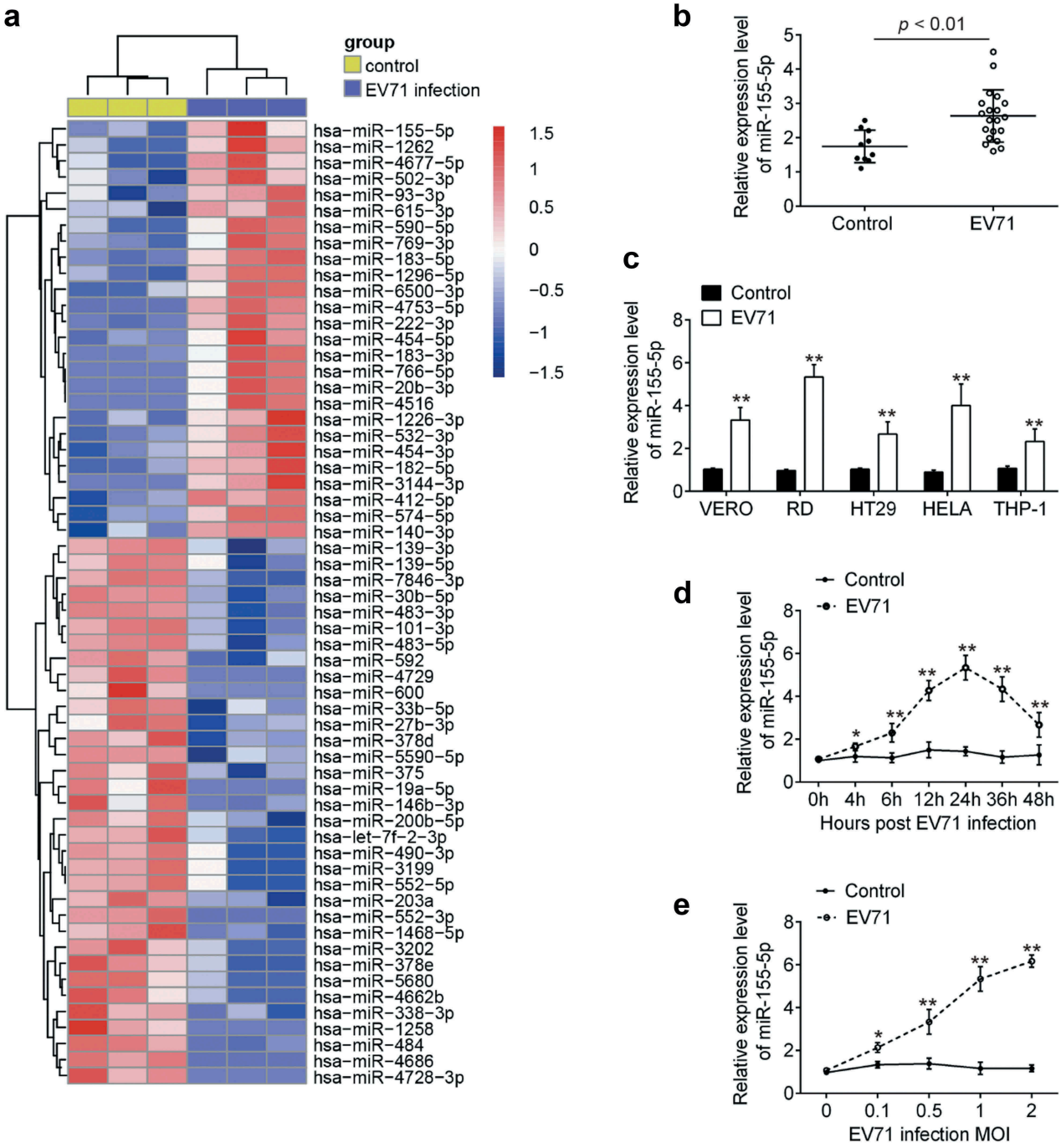


**Figure 1.** MiR-155-5p is upregulated in serum from EV71 infected patients and EV71-infected cell lines. (a) Heat map analysis of the microRNA expression between serum samples from EV71-infected patients and healthy controls (n = 3). (b) qRT-PCR was performed to measure the levels of miR-155-5p in 20 serum samples from EV71-infected patients and 10 serum samples from healthy controls. $p < 0.01$ *vs*. Control group. (c) The expression of miR-155-5p was detected by qRT-PCR in EV71-infected cell lines, including Vero, RD, HT-29, HeLa, and THP-1 cells. (d) Expression of miR-155-5p was determined in RD cells at the different times (0, 4, 6, 12, 24, 36, and 48 h) after EV71 infection. (e) Expression levels of miR-155-5p were determined in RD cells at 24 h after different dose of EV71 (0, 0.1, 0.5, 1 and 2 MOI) infection. Data are the mean ± S.D. (n = 3) of one representative experiment. *p < 0.05, **p < 0.01 vs. control group.

infection. The results showed that overexpression of miR-155-5p significantly reduced EV71 titers, while knockdown of miR-155-5p promoted EV71 titers, compared to respective NC group (Figure 2(b,c)), these effects was time-dependent. EV71 virion protein 1 (VP1) is the most external, surface-accessible, and immunodominant protein, which is involved in the process of viral entry [31,32]. Thus, we assessed the

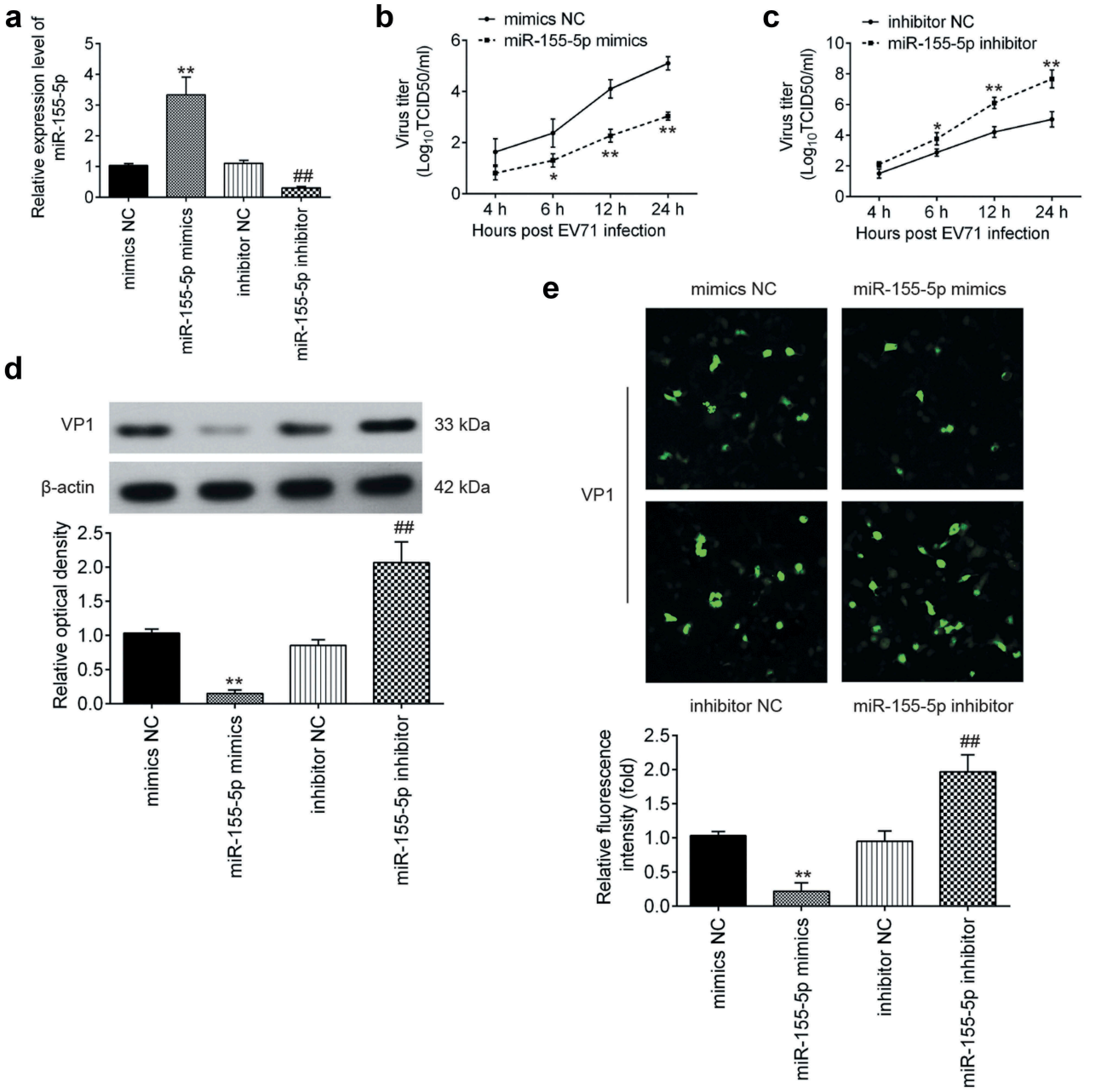


**Figure 2.** MiR-155-5p regulates EV71 replication. miR-155-5p mimics and its inhibitor were added into RD cells for 24 h, and then the cells were infected with EV71 (MOI = 1) for 24 h. (a) Expression of miR-155-5p was determined by qRT-PCR. (b, c) EV71 titers were measured by $TCID_{50}$ assay. (d) VP1 protein expression level was detected by Western blot analysis and blot bands were semi-quantified with ImageJ version 1.46. (e) VP1 protein expression level was detected by immunofluorescence assay. (200 × magnification). ImageJ version 1.46 was used to quantify IFA. Data are the mean ± S.D. (n = 3) of one representative experiment. $^{**}p < 0.01$ *vs*. mimics NC group; $^{\#\#}p < 0.01$ *vs*. inhibitor NC group.

effect of miR-155-5p on the expression levels of VP1 in EV71 infected RD cells. The results showed that miR-155-5p overexpression markedly reduced the expression of VP1, whereas miR-155-5p inhibition led to a significant increase in the expression of VP1, compared with that in the respective negative-control groups (Figure 2(d)). Immunofluorescence assay also showed that the expression of VP1 was significantly decreased by miR-155-5p overexpression, but increased by miR-155-5p inhibition (Figure 2(e)). Collectively, these data reveal the antiviral activity of miR-155-5p during EV71 infection.

### *miR-155-5p regulated the production of type I IFNs*

It is well-known that innate immune response, especially type I IFNs play important roles in limiting EV71 replication [8,33]. To elucidate the mechanisms that miR-155-5p affects EV71 replication, the RD cells were transfected with miR-155-5p mimics or inhibitor, followed by infection with EV71 at an MOI of 1. The expressions of IFNα/β were examined by ELISA assays. Overexpression of miR-155-5p significantly enhanced the production of EV71-induced IFNα/β, whereas knockdown of miR-155-5p inhibited these processes (Figure 3(a,b)). Further, we test the expression levels of four important IFN-stimulated genes (ISGs), including ISG15, MxA, OAS, and PKR. The mRNA levels of these ISGs in cells infected with EV71 were markedly increased after miR-155-5p mimics transfection, while reduced after miR-155-5p inhibitor transfection. These data indicate that miR-155-5p regulated the type I IFN response and affected its downstream pathway in response to EV71 infection.

### *FOXO3 was a direct target of miR-155-5p*

Through bioinformatics prediction using TargetScan 7.0 and miRanda, we found a putative target site of miR-155-5p in the 3′-UTR of FOXO3 mRNA (Figure 4(a)). FOXO3 has previously been reported to suppress the type I IFN response in several virus diseases [34–36]. Thus, FOXO3 was chose for the subsequent research. Western Blot analyzes demonstrated that FOXO3 was decreased in miR-155-5p mimics transfected RD cells, while increased in miR-155-5p inhibitor transfected RD cells (Figure 4(b)). To validate the possibility that FOXO3 was a direct target of miR-155-5p, luciferase reporter assay was

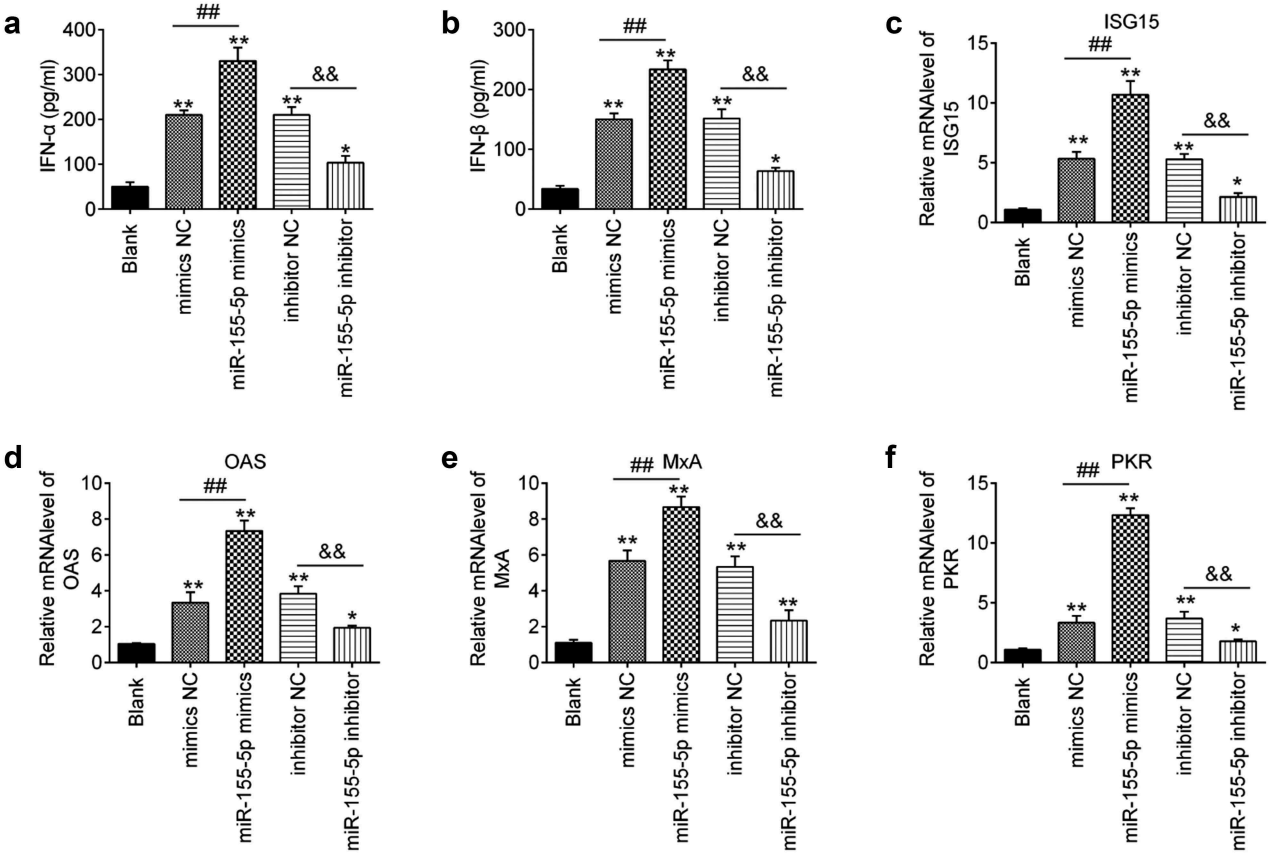


**Figure 3.** MiR-155-5p regulates the production of type I IFNs. miR-155-5p mimics and its inhibitor were transfected into RD cells for 24 h, and then the cells were infected with EV71 (MOI = 1) for 24 h. (a, b) The expressions of IFN-α/β were measured by ELISA. (c–f) Expressions of IFN-stimulated genes (ISGs), ISG15, OAS, MxA and PKR were measured by qRT-PCR. Data are the mean ± S.D. (n = 3) of one representative experiment. *$p < 0.05$, **$p < 0.01$ *vs*. control group; ##$p < 0.01$ *vs*. mimics NC group; &&$p < 0.01$ *vs*. inhibitor NC group.

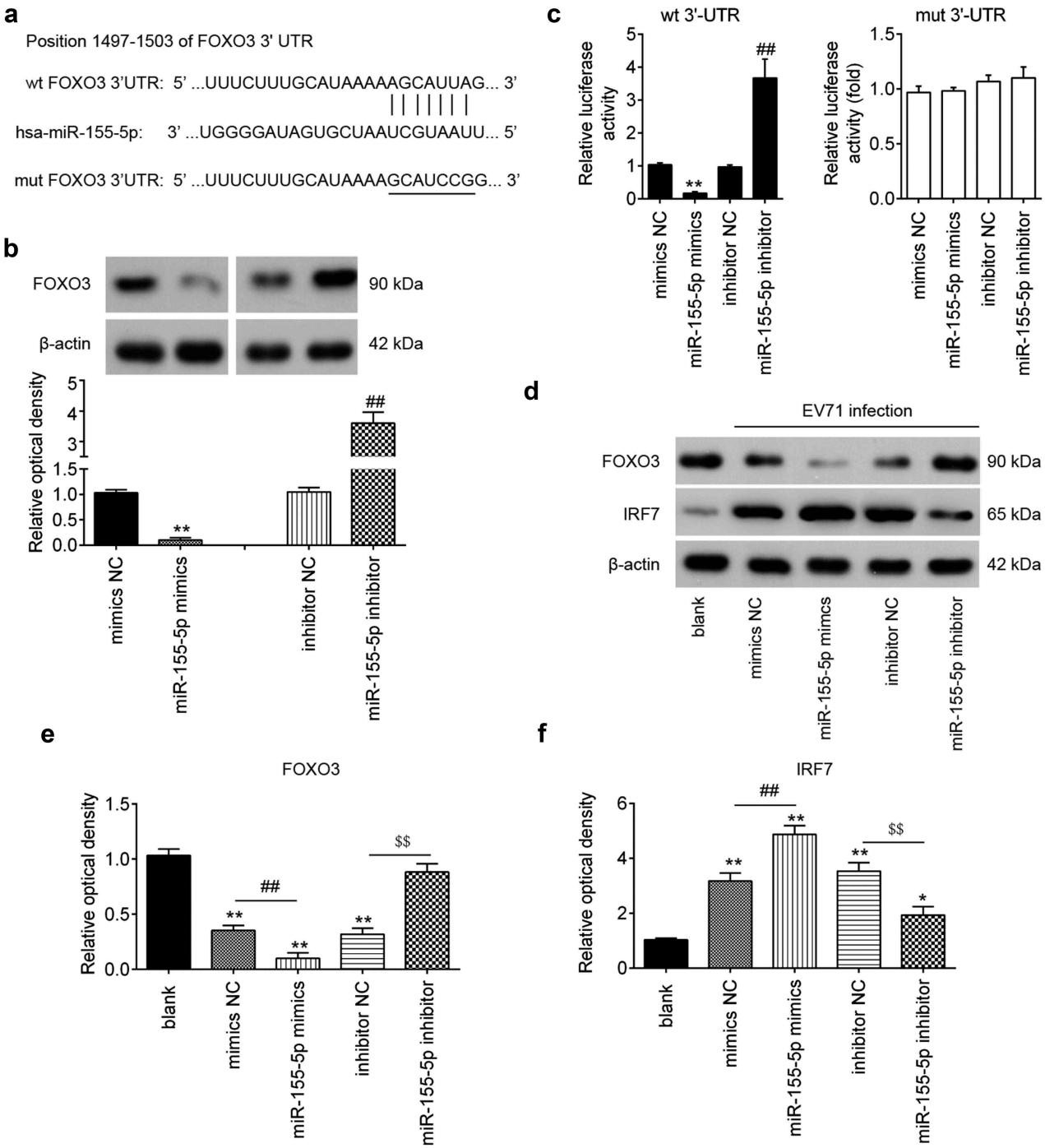


**Figure 4.** FOXO3 is a direct target of miR-155-5p. (a) The putative binding site of miR-155-5p and FOXO3 is shown. (b) The expression levels of FOXO3 protein after transfection with miR-155-5p mimics or miR-155-5p inhibitor were measured by Western blot. (c) Luciferase activity of RD cells was detected by a dual luciferase assay. Data are the mean ± S.D. (n = 3) of one representative experiment. $^{**}p < 0.01$ *vs.* mimics NC or inhibitor NC. (d) miR-155-5p mimics and its inhibitor were added into RD cells for 24 h, and then the cells were infected with EV71 (MOI = 1) for 24 h, and then the expression levels of FOXO3 and IRF7 protein were measured by Western blot and (e, f) blot bands were semi-quantified with ImageJ version 1.46.

performed. The assay revealed that the miR-155-5p mimics markedly inhibited the luciferase activity in the FOXO3-3′UTR wt reporter, and that the miR-155-5p inhibitor caused an increased luciferase activity; however, no changes were observed in the cells co-transfection of FOXO3 3'-UTR-mut with miR-155-5p (Figure 4(c)). It is well-known that FOXO3 acts as a negative regulator of IRF7, which is

an important transcriptional regulator of type I IFN response [36,37]. Thus, we sought to determine whether miR-155-5p regulates FOXO3/IRF7 axis during EV71 infection. As expected, EV71 infection in RD cells increased the expression of IRF7 and decreased the expression of FOXO3 compared to non-infected cells. Further increased IRF7 and decreased FOXO3 expressions were observed after miR-155-5p mimics transfection, indicating overexpression of miR-155-5p can further activate the FOXO3/IRF7 signaling pathway (Figure 4(d–f)). However, miR-155-5p inhibitor transfection had an opposite result (Figure 4(d–f)), suggesting that miR-155-5p regulates IRF7 expression by targeting FOXO3 in RD cells.

### *miR-155-5p inhibition promoted EV71 replication by targeting FOXO3/IRF7 pathway*

To determine whether FOXO3 participates in the effect of miR-155-5p on EV71 replication in RD cells, si-FOXO3 and miR-155-5p inhibitor were co-transfected into RD cells, followed by infection with EV71 (MOI = 1). As shown in Figure 5(a), si-FOXO3 -1 was more effective in knocking down FOXO3 than other si-FOXO3, thus si-FOXO3-1 was chose for subsequent experiments. Moreover, we found that miR-155-5p inhibition increased the EV71 titers and the expression of EV71 VP1 in RD cells, whereas knockdown of FOXO3 attenuated the enhancement of miR-155-5p inhibition in virus titers and the expression of VP1 (Figure 5(b,c)). It was also observed that miR-155-5p inhibition reduced the production of IFNα/β in EV71-infected RD cells; however, these effects of miR-155-5p inhibition were attenuated by FOXO3 knockdown (Figure 5(d,e)). Meanwhile, FOXO3 knockdown reversed the inhibitory effects of miR-155-5p inhibitor on the expression of four ISGs (ISG15, OAS, MxA and PKR) in RD cells (Figure 5(f–i)). These results suggest that miR-155-5p inhibition facilitates EV71 replication through suppression of type I IFN response by targeting FOXO3.

### *miR-155-5p inhibition promoted EV71 replication by regulating the type I IFN response* in vivo

To further determine the regulatory role of miR-155-5p *in vivo*, a mouse-adapted EV71 strain (mEV71) was generated as previously described [24]. As shown in Figure 6(a), the expressions of miR-155-5p in mice were time-dependently increased or decreased after agomir-155-5p or antagomir-155-5p injection. Interestingly, it was observed that agomir-155-5p obviously improved the survival rates, whereas antagomir-155-5p had much lower survival rates following EV71 infection compared with that in the control group (Figure 6(b)). It was also observed that agomiR-155-5p significantly reduced the mRNA of VP1 in the highly susceptible organs, particularly the brain, liver, muscle and spleen, whereas anagomiR-155-5p enhanced the mRNA expressions of VP1 (Figure 6(c)). Infection with EV71 results in encephalomyelitis, pulmonary edema, poliomyelitis-like paralysis or even neurological and psychiatric complications, in addition to HFMD [38,39]. Thus, brain and lung tissues were collected for assessment of the mRNA expression of VP1 by IHC. The results showed that VP1 expression was much higher in EV71 group than that in control group, but the VP1 expression was even lower in agomir-155-5p group compared with that in EV71 group. In the contrast, the VP1 expression was much higher in anagomir-155-5p group compared with that in EV71 group (Figure 6(d,e)). More importantly, we found a significantly increase in IFN-α/β secretion in serum after EV71 infection, compared with those in the control group. Agomir-155-5p treatment enhanced EV71 induced IFN-α/β secretion, whereas antagomir-155-5p dramatically reduced EV71 induced IFN-α/β secretion (Figure 6(f,g)). All data indicate that miR-155-5p inhibition promoted EV71 replication by the regulation of the type I IFN response in vivo.

## Discussions

Our data revealed that miR-155-5p was upregulated in response to EV71 infection. Functional analyses indicated that overexpression of miR-155-5p inhibited EV71 replication, while inhibition of miR-155-5p promoted EV71 replication in RD cells. Notably, the antiviral activity of miR-155-5p through regulating type I IFN by targeting FOXO3/IRF7 pathway was confirmed *in vitro* and *in vivo*. These findings suggest that the upregulation of miR-155-5p offer a novel therapy strategy to inhibit EV71 infection.

Mounting evidence has reported that several other miRNAs serve as a key regulator of viral entry and replication. For example, miR-128 influenced HIV-1

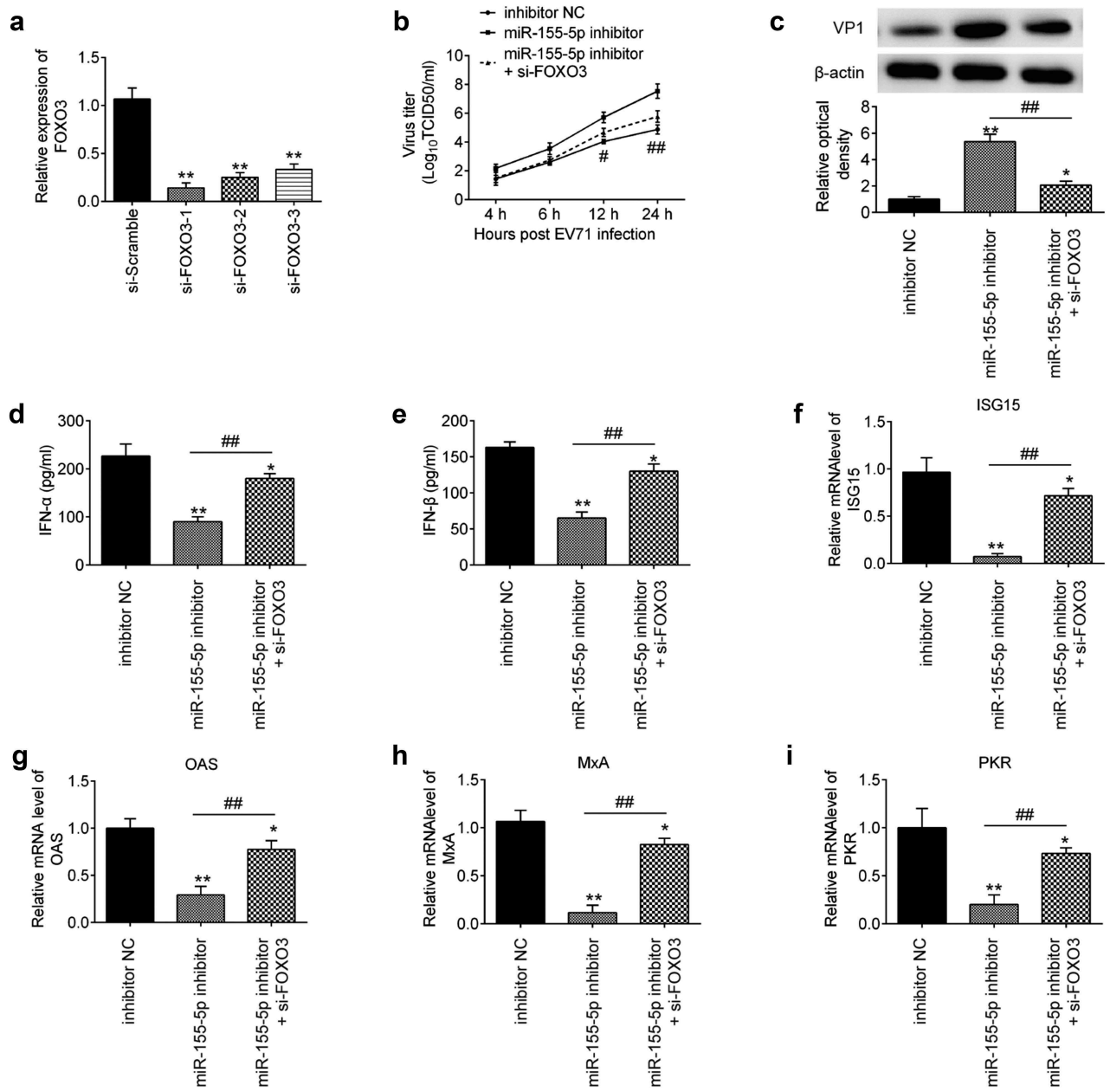


**Figure 5.** miR-155-5p inhibition promoted EV71 replication by targeting FOXO3/IRF7 pathway. (a) Transfected efficiency of si-FOXO3 was determined by Western blot. Data are presented as means of three independent experiments ± SD. $^{**}p < 0.01$ *vs*. si-scramble. (b) miR-155-5p inhibitor and si-FOXO3 were added into RD cells for 24 h, and then the cells were infected with EV71 for 24 h. The EV71 titers were measured by $TCID_{50}$ assay. Data are the mean ± S.D. (n = 3) of one representative experiment. $^{**}p < 0.01$ *vs*. inhibitor NC; $\#p < 0.05$, $\#\#p < 0.01$ *vs*. miR-155-5p inhibitor. (c) The expression of VP1 protein was detected by Western blot analysis and blot bands were semi-quantified with ImageJ version 1.46. (d, e) The expressions of IFN-α/β at protein level were measured by ELISA. Data are the mean ± S.D. (n = 3) of one representative experiment. $^{**}p < 0.01$ *vs*. inhibitor NC; $\#p < 0.05$, $\#\#p < 0.01$ *vs*. miR-155-5p inhibitor.

replication by repressing TNPO3, a factor that regulates HIV-1 nuclear import and replication [40]. Zhang et al. found that miR-146a inhibited the IRAK1/TRAF6/NF-κB signaling pathway to facilitate Borna disease virus 1 (BoDV-1) survival in host cells [41]. Wang et al. showed that inhibition of miR-194 alleviated influenza A virus (IAV)-induced lung injury by promoting type I IFN antiviral activities in mouse models [42]. In EV71 infection, miRNAs may be a double-edged sword. For example, Sun et al. found that EV71 infection increased the level of miR-545 in HEK 293 cells, and EV71 replication

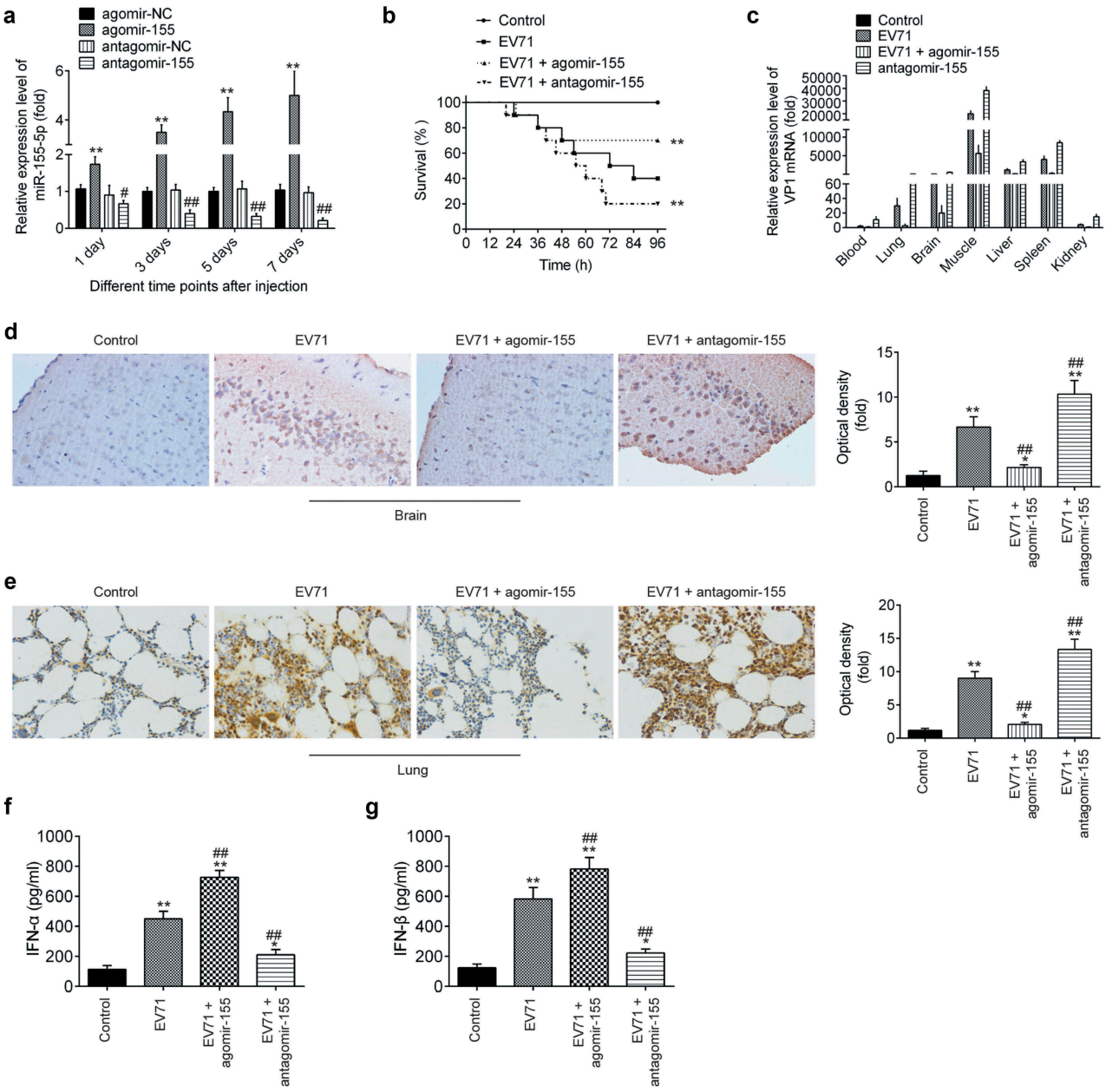


**Figure 6.** miR-155-5p inhibition promoted EV71 replication by the regulation of the type I IFN response in mice. A mouse-adapted EV71 strain (mEV71) was generated as previously described and mice were intraperitoneally injected with agomir-155-5p (1.2 mg/kg) or antagomir-155-5p (1.2 mg/kg) 24 h prior to mEV71 injection. (a) The miR-155-5p expressions were measured by qRT-PCR in EV71-infected mice by administration of agomir-155-5p or antagomir-155-5p at 1, 3, 5 and 7d post-infection. Data are the mean ± S.D. (n = 3) of one representative experiment. $^{**}p < 0.01$ *vs*. agomir-NC; $\#p < 0.05$, $\#\#p < 0.01$ *vs*. antagomir-NC. (b) Survival rates of mice with administration of agomir-155-5p or antagomir-155-5p were determined for 96 h after challenge with mEV71. $^{**}p < 0.01$ *vs*. EV71 group. (c) VP1 mRNA expression was determined by qRT-PCR at 6 days post-infection. (d, e) The protein expressions of VP1 were detected by IHC in brain and lung tissues of mice with administration of agomir-155-5p or antagomir-155-5p. ImageJ version 1.46 was used to quantify IHC staining. (f, g) IFN-α/β cytokine levels in the serum (at 6 days post-infection) were determined by ELISA. Data are the mean ± S.D. (n = 3) of one representative experiment. $^{**}p < 0.01$ *vs* control group; $\#\#p < 0.01$ *vs*. EV71 group.

was promoted by overexpression of miR-545 [43]. Another study performed by Zhao et al. reported that miR-494-3p promoted EV71 replication by directly targeting PTEN [2]. Interestingly, Wen et al. found that upregulation of miR-23b suppressed EV71 titers and EV71 VP1 protein expression [44]. Li et al. showed that miR-9-5p exerted an anti-EV71 effect in cells and a mouse model through regulation of the RIG-I-mediated innate immune response [23]. In this study, using miRNA microarray profiling and qRT-

PCR assays, miR-155-5p was one of the most significantly upregulated miRNAs in the serum of EV71 infected patients, as well as in several EV71 infected cell lines. Furthermore, overexpression of miR-155-5p reduced EV71 replication, while downregulation of miR-155-5p enhanced viral replication, as determined by the titers of EV71 and the expressions of VP1 protein. Taken together, our data demonstrated that the miR-155-5p negatively regulate the EV71 replication in RD cells.

It has been well accepted that IFN-I (IFN-α/β) play a crucial role in host antiviral responses. Once viral infection, host cells react quickly to the invading viruses by synthesizing and secreting IFN-I. After binding to its receptor (interferon alpha/beta receptor [IFNAR]), secreted IFN-I will activate downstream JAK-STAT signaling pathways, consequently up-regulating the expression of ISGs that are executors in the clearance of viral pathogens [45,46]. Notably, several studies have shown that antiviral functions in IFN-I are finely regulated by miRNAs. For example, Zhang et al. found that miR-146a could promote influenza avian virus (IAV) replication through suppressing type I IFN response by targeting TRAF6 [47]. Chen et al. showed that miR-223 inhibited vesicular stomatitis virus (VSV) replication through promoting type I IFN production by targeting FOXO3 [14]. Recent studies reported that miR-155 could suppress infectious burse disease virus (IBDV) [29] and VSV [48] replication by targeting SOCS1. However, whether or not miR-155-5p influences type I IFN response during EV71 infection remains unknown. In this study, our results showed that miR-155-5p overexpression induced the expressions of IFN-α/β and ISGs, while miR-155-5p inhibition reduced the expressions of IFNα/β and ISGs in EV71 infection RD cells and in mEV71 infected mice. All these suggest that miR-155-5p could modulate EV71 replication through regulation of type I IFN responses.

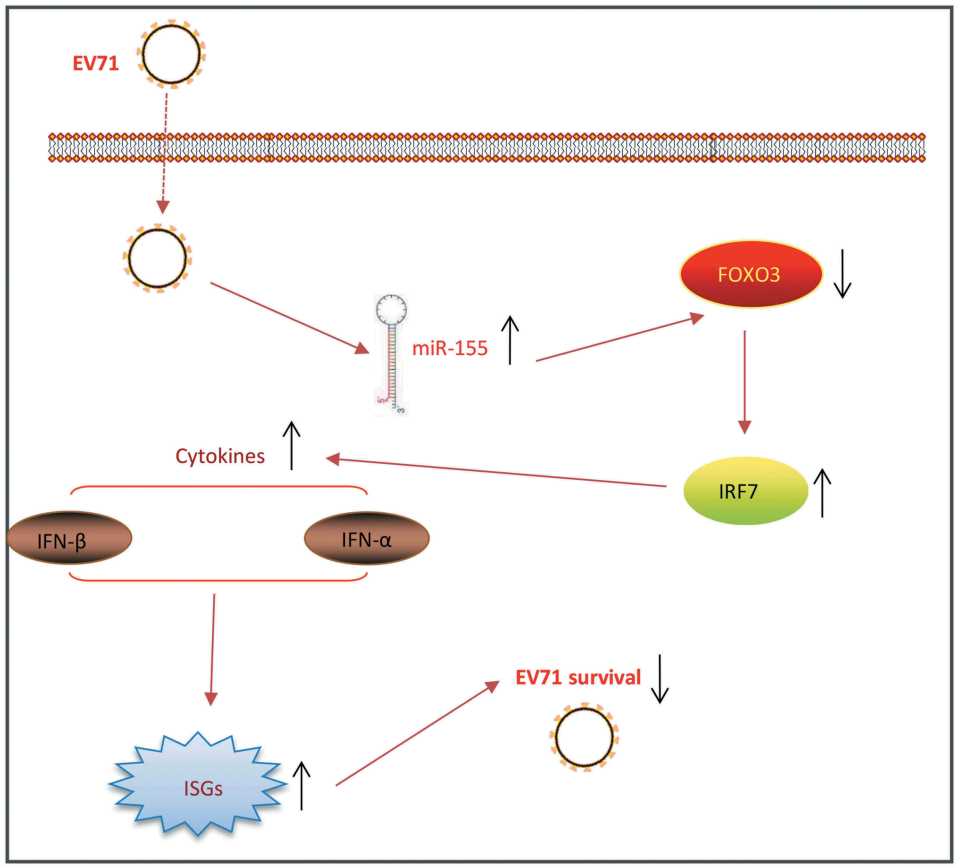


**Figure 7.** Schematic diagram of the signaling pathway in which miR-155-5p inhibits the EV71 replication. EV71 infection upregulated the expression of miR-155-5p, which increased the expression of IRF7 by targeting FOXO3, subsequently promoting type I IFN production and ISGs expressions, and thus reducing the EV71 survival.

FOXO3 functions as a negative regulator of basal IRF7 transcription, thus suppressing the IRF7-dependent antiviral response [36,49]. For example, Chen et al. observed that knockdown of FOXO3 promoted IRF7 expression and markedly increased vesicular stomatitis virus (VSV)-triggered type I IFN production in primary mouse peritoneal macrophages [14]. Another study reported that FOXO3 was a direct target of miR-182 and contributed to miR-182 mediated induction of IFN-I response and suppression of HCMV replication in neural cells [37]. Notably, previous studies showed that FOXO3 was directly targeted by miR-155 in colon cancer cells [35] and in tuberculosis [34]. However, whether FOXO3 is a target of miR-155-5p during EV71 infection remains unclear. In our study, FOXO3 was identified as a direct target of miR-155-5p in RD cells. Moreover, the promoting effects of miR-155-5p inhibitor on EV71 replication were abrogated by FOXO3 inhibition, suggesting that downregulation of miR-155-5p facilitates EV71 replication through suppression of type I IFN response by targeting FOXO3/IRF7 pathway.

In conclusion, the present study revealed that downregulation of miR-155-5p facilitates EV71 replication by diminishing type I IFN response through FOXO3/IRF7 pathway *in vitro* and *in vivo* (Figure 7). Our findings indicate that targeting FOXO3 by miR-155-5p may be an effective therapeutic strategy against EV71 infection.

## Authors contribution

Daokun Yang was responsiblefor the main conceive of the study and the draft of the manuscript. Xinwei Wang, Haili Gao, Baoxin Chen, Changyun Si and Shasha Wang helped to design the study and performed the statistical analysis. Xinwei Wang and Haili Gao helped to revise the manuscript and participated in its design. All authors have read and approved the final manuscript

## Disclosure statement

No potential conflict of interest was reported by the authors.

## References

[1] Yip CC, Lau SK, Woo PC, et al. Human enterovirus 71 epidemics: what's next? Emerg Health Threats J. 2013;6:19780.

[2] Zhao Q, Xiong Y, Xu J, et al. Host microRNA hsa-miR-494-3p promotes EV71 replication by directly targeting PTEN. Front Cell Infect Microbiol. 2018;8:278.

[3] Chan LG, Parashar UD, Lye MS, et al. Deaths of children during an outbreak of hand, foot, and mouth disease in sarawak, malaysia: clinical and pathological characteristics of the disease. For the Outbreak Study Group. Clinl Infect Dis. 2000;31:678–683.

[4] Stifter SA, Feng CG. Interfering with immunity: detrimental role of type I IFNs during infection. J Iimmunol. 2015;194:2455–2465.

[5] Killip MJ, Fodor E, Randall RE. Influenza virus activation of the interferon system. Virus Res. 2015;209:11–22.

[6] Hoffmann HH, Schneider WM, Rice CM. Interferons and viruses: an evolutionary arms race of molecular interactions. Trends Immunol. 2015;36:124–138.

[7] Chen W, Han C, Xie B, et al. Induction of siglec-G by RNA viruses inhibits the innate immune response by promoting RIG-I degradation. Cell. 2013;152:467–478.

[8] Fu Y, Zhang L, Zhang F, et al. Exosome-mediated miR-146a transfer suppresses type I interferon response and facilitates EV71 infection. PLoS Pathog. 2017;13:e1006611.

[9] Zheng C, Zheng Z, Sun J, et al. MiR-16-5p mediates a positive feedback loop in EV71-induced apoptosis and suppresses virus replication. Sci Rep. 2017;7:16422.

[10] Honda K, Yanai H, Negishi H, et al. IRF-7 is the master regulator of type-I interferon-dependent immune responses. Nature. 2005;434:772–777.

[11] Sato M, Suemori H, Hata N, et al. Distinct and essential roles of transcription factors IRF-3 and IRF-7 in response to viruses for IFN-alpha/beta gene induction. Immunity. 2000;13:539–548.

[12] He L, Hannon GJ. MicroRNAs: small RNAs with a big role in gene regulation. Nat Rev Genet. 2004;5:522–531.

[13] Yao L, Wu CX, Zheng K, et al. Immunogenic response to a recombinant pseudorabies virus carrying bp26 gene of Brucella melitensis in mice. Res Vet Sci. 2015;100:61–67.

[14] Chen L, Song Y, He L, et al. MicroRNA-223 promotes type I interferon production in antiviral innate immunity by Targeting forkhead box protein O3 (FOXO3). J Biol Chem. 2016;291:14706–14716.

[15] Ma Y, Wang C, Xue M, et al. The coronavirus transmissible gastroenteritis virus evades the type I interferon response through IRE1alpha-mediated manipulation of the microRNA miR-30a-5p/SOCS1/3 axis. J Virol. 2018;92:e00728-18.

[16] Xie Y, He S, Wang J. MicroRNA-373 facilitates HSV-1 replication through suppression of type I IFN response by targeting IRF1. Biomed Pharmacothe. 2018;97:1409–1416.

[17] Feng N, Zhou Z, Li Y, et al. Enterovirus 71-induced has-miR-21 contributes to evasion of host immune system by targeting MyD88 and IRAK1. Virus Res. 2017;237:27–36.

[18] Stanic M. A simplification of the estimation of the 50 percent endpoints according to the Reed and Muench method. Pathologia et microbiologia. 1963;26:298–302.

[19] Mei LL, Wang WJ, Qiu YT, et al. miR-125b-5p functions as a tumor suppressor gene partially by regulating HMGA2 in esophageal squamous cell carcinoma. PloS One. 2017;12:e0185636.
[20] Livak KJ, Schmittgen TD. Analysis of relative gene expression data using real-time quantitative PCR and the 2(-Delta Delta C(T)) method. Methods. 2001;25:402–408.
[21] Ren L, Zhao Y, Huo X, et al. MiR-155-5p promotes fibroblast cell proliferation and inhibits FOXO signaling pathway in vulvar lichen sclerosis by targeting FOXO3 and CDKN1B. Gene. 2018;653:43–50.
[22] Wu H, Huang T, Ying L, et al. MiR-155 is involved in renal ischemia-reperfusion injury via direct targeting of FoxO3a and regulating renal tubular cell pyroptosis. Cell Physiol Biochem. 2016;40:1692–1705.
[23] Li B, Zheng J. MicroR-9-5p suppresses EV71 replication through targeting NFkappaB of the RIG-I-mediated innate immune response. FEBS Open Bio. 2018;8:1457–1470.
[24] Wang YF, Chou CT, Lei HY, et al. A mouse-adapted enterovirus 71 strain causes neurological disease in mice after oral infection. J Virol. 2004;78:7916–7924.
[25] Ho BC, Yu IS, Lu LF, et al. Inhibition of miR-146a prevents enterovirus-induced death by restoring the production of type I interferon. Nat Commun. 2014;5:3344.
[26] Bao JL, Lin L. MiR-155 and miR-148a reduce cardiac injury by inhibiting NF-kappaB pathway during acute viral myocarditis. Eur Rev Med Pharmacol Sci. 2014;18:2349–2356.
[27] Pareek S, Roy S, Kumari B, et al. MiR-155 induction in microglial cells suppresses Japanese encephalitis virus replication and negatively modulates innate immune responses. J Neuroinflammation. 2014;11:97.
[28] Xie C, Ren GL, Xu MC, et al. The effect of miR-155 on HBV replication and PTEN expression in vivo. Zhonghua Gan Zang Bing Za Zhi. 2018;26:489–494.
[29] Wang B, Fu M, Liu Y, et al. gga-miR-155 enhances type I interferon expression and suppresses infectious burse disease virus replication via targeting SOCS1 and TANK. Front Cell Infect Microbiol. 2018;8:55.
[30] Gupta R, Arkatkar T, Keck J, et al. Antigen specific immune response in Chlamydia muridarum genital infection is dependent on murine microRNAs-155 and −182. Oncotarget. 2016;7:64726–64742.
[31] Cordey S, Petty TJ, Schibler M, et al. Identification of site-specific adaptations conferring increased neural cell tropism during human enterovirus 71 infection. PLoS Pathog. 2012;8:e1002826.
[32] Strauss M, Filman DJ, Belnap DM, et al. Nectin-like interactions between poliovirus and its receptor trigger conformational changes associated with cell entry. J Virol. 2015;89:4143–4157.
[33] Rasti M, Khanbabaei H, Teimoori A. An update on enterovirus 71 infection and interferon type I response. Rev Med Virol. 2019;29:e2016.
[34] Huang J, Jiao J, Xu W, et al. MiR-155 is upregulated in patients with active tuberculosis and inhibits apoptosis of monocytes by targeting FOXO3. Mol Med Rep. 2015;12:7102–7108.
[35] Gao Y, Liu Z, Ding Z, et al. MicroRNA-155 increases colon cancer chemoresistance to cisplatin by targeting forkhead box O3. Oncol Lett. 2018;15:4781–4788.
[36] Litvak V, Ratushny AV, Lampano AE, et al. A FOXO3-IRF7 gene regulatory circuit limits inflammatory sequelae of antiviral responses. Nature. 2012;490:421–425.
[37] He X, Teng J, Cui C, et al. MicroRNA-182 inhibits HCMV replication through activation of type I IFN response by targeting FOXO3 in neural cells. Exp Cell Res. 2018;369:197–207.
[38] Chang LY, Huang LM, Gau SS, et al. Neurodevelopment and cognition in children after enterovirus 71 infection. N Engl J Med. 2007;356:1226–1234.
[39] Huang CC, Liu CC, Chang YC, et al. Neurologic complications in children with enterovirus 71 infection. N Engl J Med. 1999;341:936–942.
[40] Bochnakian A, Zhen A, Zisoulis DG, et al. Interferon-inducible miR-128 modulates HIV-1 replication by targeting TNPO3 mRNA. J Virol. 2019;93:e00364-19.
[41] Zhang X, Guo Y, Xu X, et al. miR-146a promotes Borna disease virus 1 replication through IRAK1/TRAF6/NF-kappaB signaling pathway. Virus Res. 2019;271:197671.
[42] Wang K, Lai C, Gu H, et al. miR-194 inhibits innate antiviral immunity by targeting FGF2 in influenza H1N1 virus infection. Front Microbiol. 2017;8:2187.
[43] Sun Y, Feng L, Li J, et al. miR-545 promoted enterovirus 71 replication via directly targeting phosphatase and tensin homolog and tumor necrosis factor receptor-associated factor 6. J Cell Physiol. 2019;234:15686–15697.
[44] Wen BP, Dai HJ, Yang YH, et al. MicroRNA-23b inhibits enterovirus 71 replication through downregulation of EV71 VPl protein. Intervirology. 2013;56:195–200.
[45] Sadler AJ, Williams BR. Interferon-inducible antiviral effectors. Nat Rev Immunol. 2008;8:559–568.
[46] Schoggins JW, Rice CM. Interferon-stimulated genes and their antiviral effector functions. Curr Opin Virol. 2011;1:519–525.
[47] Zhai T, Wu C, Wang N, et al. Development of a monoclonal antibody against swine leukocyte antigen (SLA)-DR alpha chain and evaluation of SLA-DR expression in bone marrow-derived dendritic cells after PRRSV infection. Vet Immunol Immunopathol. 2019;211:19–24.
[48] Wang P, Hou J, Lin L, et al. Inducible microRNA-155 feedback promotes type I IFN signaling in antiviral innate immunity by targeting suppressor of cytokine signaling 1. J Iimmunol. 2010;185:6226–6233.
[49] Liu X, Cai X, Zhang D, et al. Zebrafish foxo3b negatively regulates antiviral response through suppressing the transactivity of irf3 and irf7. J Iimmunol. 2016;197:4736–4749.